Source to sink reconstruction of a Holocene Fjord-infill

Depositional patterns, suspended sediment yields, wind-induced circulation patterns and trapping efficiency for Lake Strynevatnet, inner Nordfjord, Norway

Storms, Joep; Beylich, Achim A.; Hansen, Louise; Waldmann, Nicolas

DOI
10.1002/dep2.101

Publication date
2020

Document Version
Final published version

Published in
The Depositional Record

Citation (APA)
Storms, J., Beylich, A. A., Hansen, L., & Waldmann, N. (2020). Source to sink reconstruction of a Holocene Fjord-infill: Depositional patterns, suspended sediment yields, wind-induced circulation patterns and trapping efficiency for Lake Strynevatnet, inner Nordfjord, Norway. *The Depositional Record*, *6*(2), 471-485. https://doi.org/10.1002/dep2.101

Received: 18 April 2019 | Revised: 12 December 2019 | Accepted: 30 December 2019

DOI: 10.1002/dep2.101

ORIGINAL RESEARCH ARTICLE

The Depositional Record Open Access
A journal of the International Association of Sedimentologists
IAS
WILEY

Source to sink reconstruction of a Holocene Fjord-infill: Depositional patterns, suspended sediment yields, wind-induced circulation patterns and trapping efficiency for Lake Strynevatnet, inner Nordfjord, Norway

Joep E. A. Storms[1] | **Achim A. Beylich**[2] | **Louise Hansen**[3] | **Nicolas Waldmann**[4]

[1]Department of Geoscience & Engineering, Delft University of Technology, Delft, The Netherlands

[2]Geomorphological Field Laboratory (GFL), Selbustrand, Norway

[3]Geological Survey of Norway, Trondheim, Norway

[4]The Dr. Moses Strauss Department of Marine Geosciences, Charney School of Marine Sciences, University of Haifa, Haifa, Israel

Correspondence
Joep Storms, Department of Geoscience & Engineering, Delft University of Technology, Delft, The Netherlands.
Email: j.e.a.storms@tudelft.nl

Funding information
Nederlandse Organisatie voor Wetenschappelijk Onderzoek, Grant/Award Number: ALW-NAP/08-06

Abstract

This paper reconstructs the sedimentation volumes and patterns, suspended sediment yields, wind-induced circulation patterns and sediment trapping efficiency of Lake Strynevatnet, western Norway as an integrated source to sink system. The lake became deglaciated *ca* 11 ky cal BP, with glacio-isostatic uplift isolating the basin from the nearby fjord (Nordfjord) *ca* 9.2 ky cal BP. Based on geophysical data collected in 2010, the upper 15–20 m of Holocene sediment accumulation in the lake was mapped. A sediment body in the centre of the lake indicates a depositional mechanism dominated by suspension sedimentation. The source of this sediment is associated with the adjacent glaciated catchments westward of the lake. Three seismic units were identified based on seismic facies generating an evolutionary model utilizing three depositional units (U1, U2 and U3), in which unit U2 represents the Storegga tsunami event. Unit U3 is further divided into three subunits; U3a, U3b and U3c based on their spatial continuity and subtle downlapping and onlapping relationships. The degree to which wind conditions could have affected the lake depositional patterns were studied utilizing an open-source coupled hydrodynamic and sediment transport model. The results show that fluvial discharge alone is incapable of generating a circulation pattern in the lake currents. Suspended sediment concentrations in the lake are highest for strong winds. Modelled sediment accumulation on the lake floor shows that mild or absent winds lead to a proximal to distal sediment thickness trend, while strong winds result in uniform sediment thickness. Based on this it is argued that the thickness trends of seismic subunits U3a-c are related to a variable palaeowind climate. As such, seismic data of lake infills, in combination with numerical modelling, may provide valuable palaeoclimatic information on wind patterns.

KEYWORDS

Glacier-fed rivers, hydrodynamic modelling, palaeowind, sediment yield, sedimentation patterns, seismic stratigraphy, suspended sediment concentration, trapping efficiency

1 | INTRODUCTION

Understanding sedimentation patterns in fjords and fjord-lake systems is important for palaeoenvironemental and palaeoclimate reconstructions. Lakes in glaciated areas provide an ideal setting to study their response to Late Holocene climate changes and glacial fluctuations. The focus of this paper is on Lake Strynevatnet, a 220 m deep lake characterized by high sediment trapping efficiency. By characterizing the sedimentary infill geometry the aim is to increase our understanding of the interaction between sedimentation rates, sediment dispersal patterns and glacier activity over the past *ca* 8150 years. The sediment dispersal patterns in Lake Strynevatnet are likely driven by wind-induced circulation patterns in the absence of other main driving forces for sediment dispersal such as large fluvial systems and slope failures. There has been little research on the effects of palaeowind conditions on Holocene lake sedimentation.

Reconstructions of lake sedimentation using seismic data allows a detailed view of the shifts in sediment thickness and volume, sedimentary patterns and sediment yield with changing glacial conditions. The objective of this paper is therefore to reconstruct the long-term suspended sediment budget in Lake Strynevatnet based on geophysical measurements and to gain insight into the effects of temporal deglaciation of the Jostedalsbreen ice cap on the infill pattern. In this contribution, the focus is only on suspended sediments as these usually travel furthest in a lacustrine system. Bedload from the rivers that drain the glaciers is typically coarse-grained and limited to the delta foresets, which very locally develop in Lake Strynevatnet (Hansen *et al.*, 2009; Beylich and Laute, 2015).

Research questions that are addressed here include: (a) How much suspended sediment did the lake basin catchment produce during the Holocene? (b) How did the infill change throughout deglaciation of the Jostedalsbreen ice cap? (c) Does the infill pattern indicate changes in dispersal modes? (d) How do the long-term average suspended sediment flux values compare to contemporaneous measurements?

2 | RESEARCH AREA

2.1 | Physiography

Lake Strynevatnet is a freshwater lake located at the head of the 110 km long Nordfjord fjord (Figure 1). The physiography of Lake Strynevatnet is characterized by a typical fjord-like geometry that includes up to 1,000 m high steep valley walls and a U-shaped basin floor. With a total area of 21.6 km^2, its maximum depth is approximately 220 m, its median width is 2 km and it reaches 13.7 km in length. A shallow lake (Nerfloen; less than 10 m deep) connects the western effluent of Lake Strynevatnet to Nordfjord, continuing into a 10 km long and 500–1,000 m wide valley that is characterized by a meandering fluvial system. The catchment of Lake Strynevatnet is 440 km^2 in extent, of which 16% to 18% is presently glaciated (Vasskog *et al.*, 2012), including four wide valley systems that jointly represent 370 km^2 of the entire catchment. While two of these valleys (Erdalen and Sunndalen) are

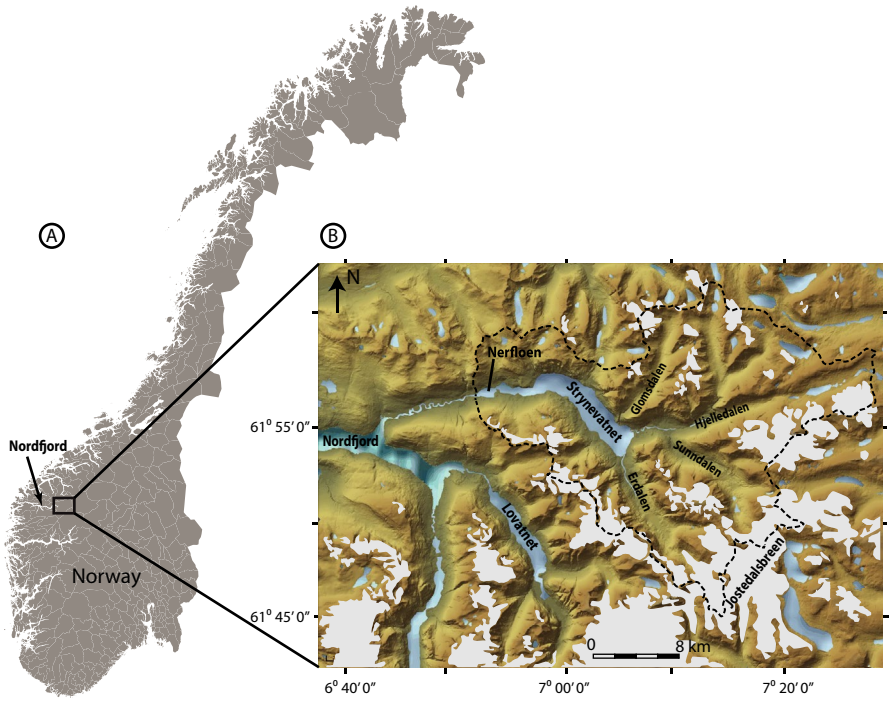

FIGURE 1 Location map of the research area. (A) Map of Norway marking the Nordfjord site. Open black square marks the location of (B). (B) A detailed shaded relief map of the Strynevatnet area (obtained from www.norgeskart.no). The dotted line represents the catchment area of the lake (redrawn from Vasskog *et al.*, 2012). Present day glaciers and ice sheets are drawn in white

presently connected to the Jostedalsbreen ice sheet, the other two are mostly affected by fringing glaciers (Hjelledalen and Glomsdalen) (Figure 1). Sunndalen and Hjelledalen merge 3.5 km upstream of their effluent. Of these valley systems, sediment and water discharges of Erdalen were monitored between 2004 and 2015 (Figure 2; Beylich et al., 2009, 2017; Beylich and Laute, 2012, 2015). The contemporary water discharge from Erdalen is low (on average 3.5 m^3/s), while peak flow can reach up to 30 m^3/s (Beylich *et al.*, 2017). The Erdalen catchment area encompasses 79.5 km^2 and consists of a series of small basins and connecting braid plains descending from the Jostedalsbreen ice sheet. The Erdalen River builds a coarse-grained delta in the southernmost part of Lake Strynevatnet (Beylich and Laute, 2015). Between 2004 and 2015 daily discharge-weighted suspended sediment concentrations were calculated from hourly readings of optical turbidity at four stationary hydrometric stations in Erdalen using turbidity sensors (Global Water), in combination with frequent direct water sampling. From these measurements, a mean annual suspended sediment yield is calculated for the Erdalen drainage basin (16.4 t/km^2/year). Contemporary suspended sediment transport accounts for almost two-thirds of the total fluvial transport and, accordingly, plays an important role within the sedimentary budget of the Erdalen drainage basin as well as for the suspended sediment supply to Lake Strynevatnet (Beylich *et al.*, 2017).

2.2 | Deglaciation history and sediment storage

Nordfjord is one of the major fjord systems in Western Norway in which a detailed glacial and deglacial history has been well-documented (Aarseth *et al.*, 1989; Nesje *et al.*, 1991; Nesje and Kvamme, 1991; Aarseth, 1997; Nesje *et al.*, 2000; Hjelstuen *et al.*, 2009; Lysså *et al.*, 2010). At the head of Nordfjord, a series of lakes developed after the area deglaciated as a result of glacio-isostatic uplift. Lake Strynevatnet deglaciated *ca* 11000 cal yr BP during the Preboreal interval (Rye *et al.*, 1997; Hjelstuen *et al.*, 2009; Nesje, 2009; Lysså *et al.*, 2010). It became a freshwater lacustrine environment *ca* 9200 cal yr BP as glacio-isostatic uplift raised the basin and disconnected it from the fjord environment (Vasskog *et al.*, 2012). The Jostedalsbreen ice cap melted between 7300 and 6100 cal yr BP (Nesje *et al.*, 2000; Nesje, 2009), which was followed by regrowth *ca* 4000 cal yr BP. This latter interval, which is referred to as the Neoglacial event, eventually led to a glacial maximum during the Little Ice Age *ca* 1750 AD (Nesje, 2009). The glacier history is reflected in the infill pattern of a series of upstream valley basins in Erdalen, with a total sediment storage capacity of *ca* 50×10^6 m^3 (Hansen *et al.*, 2009). A number of studies have constrained the sediment budgets of Nordfjord, with estimates pointing to *ca* 25 km^3 of sediments stored within the entire Nordfjord Basin (Hjelstuen *et al.*, 2009). Previous geophysical studies, accompanied by shallow piston cores in Lake Strynevatnet and in the nearby Nerfloen, Lovatnet and Oldevatnet lakes identify Holocene climate oscillations (Waldmann *et al.*, 2007). Other investigations record the 8150 cal yr BP Storegga tsunami event in the shallow basin fill (Vasskog *et al.*, 2013).

FIGURE 2 Picture of the Erdalen valley taken from Lake Strynevatnet. The U-shaped valley and steep walls of the lake are well defined

3 | METHODOLOGY

3.1 | Parametric echosounder survey

In summer 2010 a 2-week geophysical campaign was conducted to collect echosounder data in lakes Strynevatnet and Nerfloen using a parametric echosounder system (PES) developed by Innomar Technologies GmbH, which is a portable alternative to chirp and boomer sourced geophysical systems. A total of *ca* 100 km of high-quality geophysical data was collected in Lake Strynevatnet using the PES mounted to a 4.5 m inflatable boat powered by a small outboard motor. Navigation and positioning was provided by GPS. Data collection was constrained by wave heights <0.2 m.

The PES uses non-linear sound pulses that are transmitted in the water body and reach the lake floor (Wunderlich and Muller, 2003). The transducer transmits two slightly different simultaneous frequencies, which interact in the water column. A new secondary frequency, ranging between 4 and 15 kHz, is generated from the different frequencies of the primary transmitted waves and this is low enough to penetrate the subsurface sediments. However, the primary-frequency signals (about 100 kHz) can be used to determine the water depth. The parametric approach results in a narrow secondary sound beam (±1.8°) with a footprint of about 13 m at 220 m water depth, and smaller footprint at shallower depths. On average, the number of pulses per second ranges between 10 and 15, depending on the water depth and the recording window of the receiver. Four or five pulses per ping were used to increase the signal-to-noise ratio. The reflected signals are used

to calculate an echo print showing the sub-bottom structures along the sailed track. The obtained two way travel-time can be converted into depth based on an assumed sound speed in unconsolidated, fine-grained sediments of 1,500 m/s (which is in the range of values used in similar studies by Mullins *et al.*, 1991; Van Rensbergen *et al.*, 1998; Chapron *et al.*, 2007; Fanetti *et al.*, 2008; Waldmann *et al.*, 2010; Cukur *et al.*, 2015; Schneider von Deimling *et al.*, 2016), in the absence of local velocity measurements. The echo strength depends on the reflection coefficient, the attenuation of the signal and the roughness of the lake floor. The penetration depth is mainly controlled by sediment parameters (e.g. roughness and attenuation), sub-bottom profiling properties (e.g. source level), secondary frequency and by environmental conditions (e.g. noise originating from the vessel engines).

3.2 | Geophysical data treatment and interpretation

The geophysical data were interpreted using the dedicated PES software ISE (version 2.9.5 from Innomar Technologie GmbH). The GPS data were visualized and analysed using Fugawi Global Navigator software version 4.5. The interpreted sub-bottom and lake floor reflectors were exported to Surfer Version 8 (developed by Golden Software) and interpolated into surfaces on a 100 m^2 grid using triangulation with linear interpretations (anisotropic ratio of 1 and an angle of 320°). These surfaces were used to determine bathymetry and thickness and to calculate sediment volumes.

3.3 | Delft3D model

Data was processed using Delft3D (version 4.02), which is an open-source software package developed by Deltares designed to simulate three dimensional hydrodynamics, sediment fluxes and morphologic changes in fluvial, lacustrine and marine settings (Lesser *et al.*, 2004; Hillen *et al.*, 2014; van der Vegt *et al.*, 2016).

4 | RESULTS

The geophysical data resulted in three long E–W profiles (following the lake main axis) and 13 transverse profiles perpendicularly crossing the lake long axis (Figure 3).

4.1 | Bathymetry

In the absence of available bathymetric data for Lake Strynevatnet geophysical profiles were used to construct a bathymetric map (Figure 3). The map shows steep valley sidewalls (typically between 15° and 30°) and a flat lake floor with a maximum depth of *ca* 220 m.

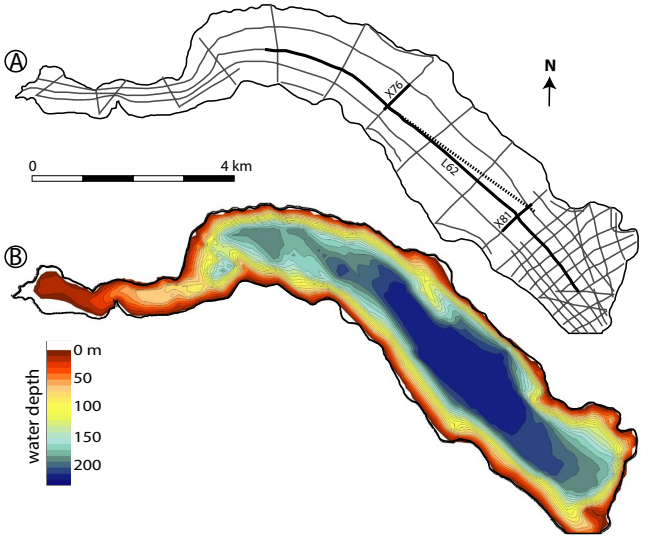

FIGURE 3 (A) Location of the acquired geophysical data (the tracks in bold black lines are shown in Figures 4 and 5). (B) Bathymetry of Lake Strynevatnet as interpolated from the geophysical data (see text for further details). The dashed black line represents the location of the seismic profile published in Vasskog *et al.* (2013), see Figure 4B

4.2 | Seismic stratigraphy and facies definition

The lake sidewalls were mostly bare of sediment, most likely due to their steep angles. Based on seismic facies interpretation, three main seismic units are identified below the lake floor (U1–U3; Figures 4 and 5). The units are described as follows:

- Seismic unit U1 consists of faint and slightly undulating non-continuous parallel to sub-parallel reflectors. Occasionally, some local inclined internal reflectors characterize the unit (e.g. in profile X81; Figure 5). The unit base is most often unidentified in the seismic profiles due to local strong attenuation of the signal by the overlying sediments. Nevertheless, when occasionally visualized, it is recognized as a clear undulating reflector especially in the north-west area of the lake. The thickness of unit U1 can reach up to 5 m. The upper boundary of unit U1 is typically continuous and less undulating than the lower boundary.
- Seismic unit U2 consists of a seismically transparent unit up to 4 m thick, with clear upper and lower reflectors. Unit U2 is imaged consistently throughout the basin and its thickness varies between 1.5 and 3.5 m. The upper boundary of unit U2 is commonly very well expressed as a strong continuous and sub-horizontal reflector.

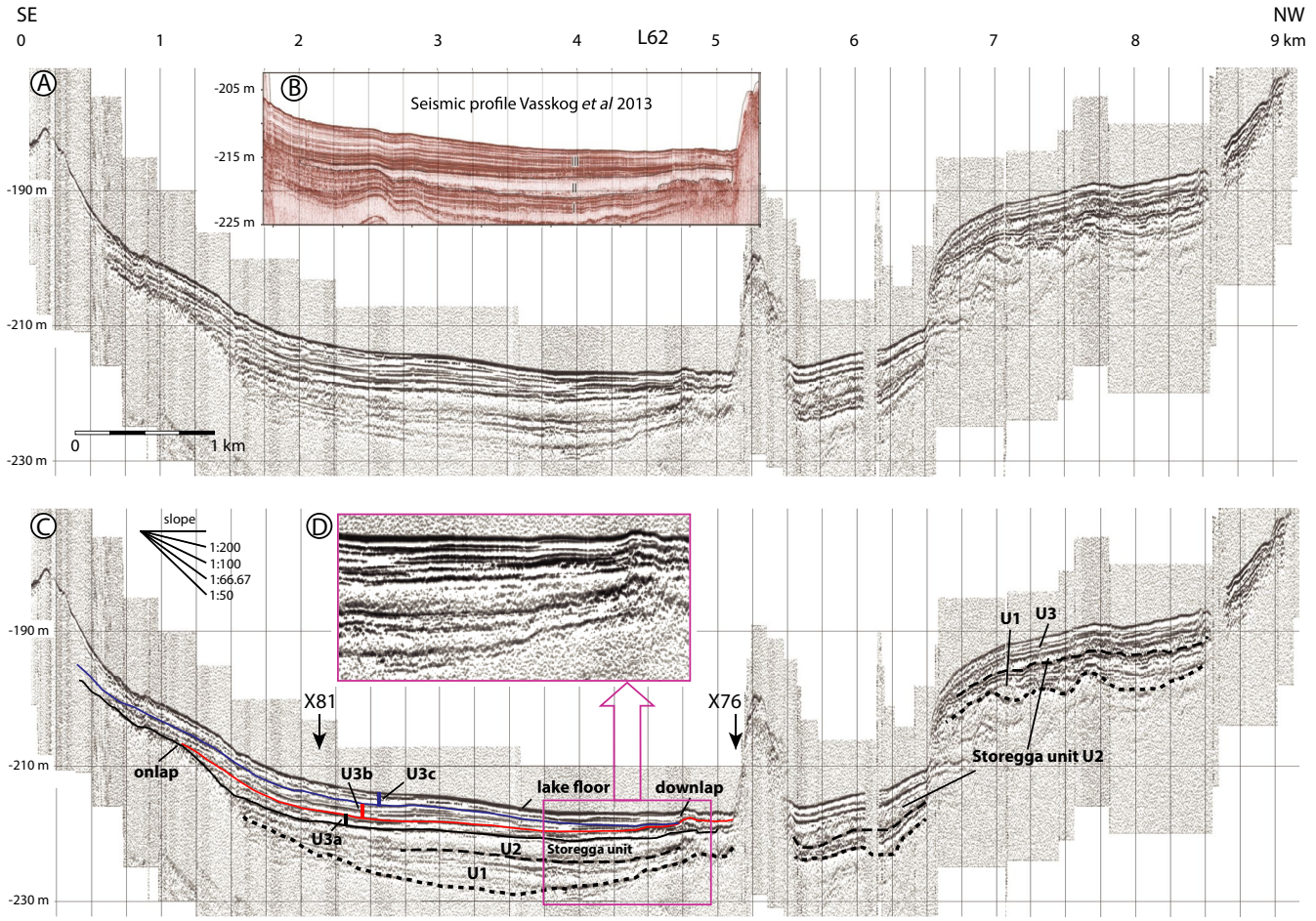

FIGURE 4 Density plots showing the raw data (A) and the interpretation (C) of profile L62 using the Parametric Echosounder (see Figure 3 for location). (B) A previously published seismic profile (Vasskog et al., 2013) at a location slightly north-east of profile L62. The interpreted seismic units by Vasskog *et al.* (2013) compare well with this papers interpretation of profile L62. The top of the Storegga deposit (black line), top of U3a (red line) and top of U3b (blue line) are interpreted as shown. Underlying deposits (U1 and U2) are denoted by black dotted lines. Only the lake infill is shown, not the steep lake side slopes. The inset (D) shows the pinch out of U3b in more detail

- Seismic unit U3 consists of thin, parallel to sub-parallel sub-horizontal reflectors with a thickness ranging between 2 and 7 m. The continuity and amplitude of reflectors varies within unit U3. Strong reflectors are commonly very continuous while thin reflectors with lower amplitude are less continuous (Figures 4 and 5). Overall, this unit thins towards the north-west. Unit U3 can be further divided into three subunits: U3a, U3b and U3c based on their spatial continuity and subtle downlapping and onlapping internal relationships (Figures 4 and 5). While units U3a and U3c are relatively uniform in thickness, the thickness of unit U3b decreases towards the north-west.

4.3 | Thickness trends of stratigraphic units

Based on the geophysical interpretation of key reflectors, isopach maps have been constructed utilizing the base and top of unit U1 and the tops of units U2, U3a, U3b and U3c (when visible). It should be taken into consideration that estimates do not include thicknesses thinner than 0.3 m due to resolution constraints. In addition, there are uncertainties associated with estimating the thicknesses of individual units (e.g. seismic interpretation and velocity uncertainties) as well as gridding (e.g. interpolation uncertainties). Combining these caveats, it is estimated that the resulting calculations point to a ±20% error.

The thicknesses of the seismic units were calculated based on the interpreted surfaces (Figure 6). The sediment thickness of seismic unit U1 and U2 reaches up to 8 m, thickening towards the sediment main source areas of Erdalen and Hjelledalen. The sediment thickness of seismic unit U3 ranges between 2 and 7 m and thins westwards, away from the main source areas. The thickest sediment package of unit U3 is identified in the deepest part of Lake Strynevatnet. However, the thickness trends of subunits U3a, U3b and U3c are markedly different and vary across

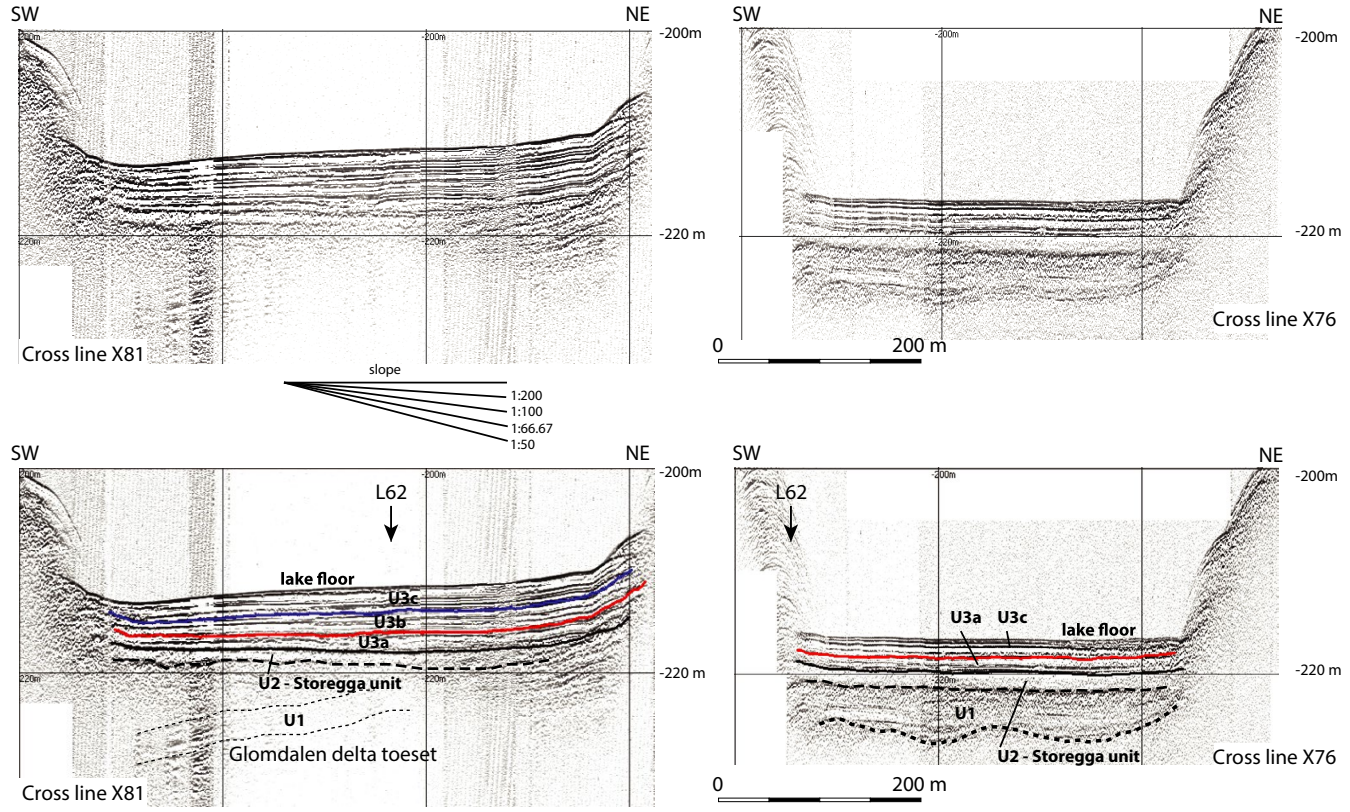

FIGURE 5 Density plots showing the raw data (upper figures) and the interpretations (lower figures) of two cross-sections X81 and X76 using the Parametric Echosounder (see Figure 3 for locations). The interpreted tops of each unit are as follows; Storegga deposit (black line), top U3a (red line) and top U3b (blue line). Underlying deposits (U1 and U2) are denoted by black dotted lines. Only the lake infill is shown, not the steep lake side slopes. The inset shows the pinch out of U3b in more detail

the lake. Unit U3a is about 1.5 m thick and generally uniform across the lake, except for thinning near Erdalen and Hjelledalen. Subunit U3b, however, has a distinct increase in thickness towards the Erdalen source area, ranging from 0 to 3 m. Subunit U3c has a relatively uniform thickness, ranging between 2 to 3 m from south-east to north-west. There is little variation in thickness perpendicular to the valley walls.

4.4 | Sediment volumes

The isopach maps have allowed the preserved sediment volumes to be calculated for the individual units and subunits. The total minimum volume of sediments mapped in Lake Strynevatnet equals 0.0537 km^3. The sum of unit U1 and U2 represents 55% of this volume (0.0293 km^3), while unit U3 represents the remaining 45% (0.0244 km^3). From the latter, subunits U3a, U3b and U3c represent 21%, 31% and 48%, respectively.

The volume of unit U2 will likely represent reworked material from the underlying unit U1 complemented with sediments that were brought to Lake Strynevatnet from Nordfjord by the Storegga tsunami.

5 | AGE CONTROL AND SEISMIC STRATIGRAPHY INTERPRETATION

A major age anchor used to constrain the sediment yield calculations in this study is based on a sedimentary unit related to the Storegga tsunami event (Bondevik *et al.*, 1997; Haflidason *et al.*, 2005). The specific character of the transparent double reflector in this study closely matches the reflector assigned to the Storegga event (Figure 4; Vasskog *et al.*, 2013). This bed was dated to 8150 cal yr BP by Vasskog *et al.* (2013). A second well constrained age is the onset of marine deposition following the deglaciation of Lake Strynevatnet calculated to *ca* 11000 cal yr BP (Waldmann *et al.*, 2007; Vasskog *et al.*, 2012). Based on this chronology the following interpretation is proposed for the lake architecture:

- Unit U1 was likely deposited after the basin was fully deglaciated *ca* 11000 cal yr BP, supporting the findings of Waldmann *et al.* (2007). During this period, glacier tongues retreated from the Strynevatnet Basin to the surrounding valleys (Rye *et al.*, 1997; Nesje, 2009). Unit U1 is especially well observed in profile X76 (Figure 5), where the undulating lower boundary of the unit reflects the palaeomorphology of the basin floor with sub-horizontal

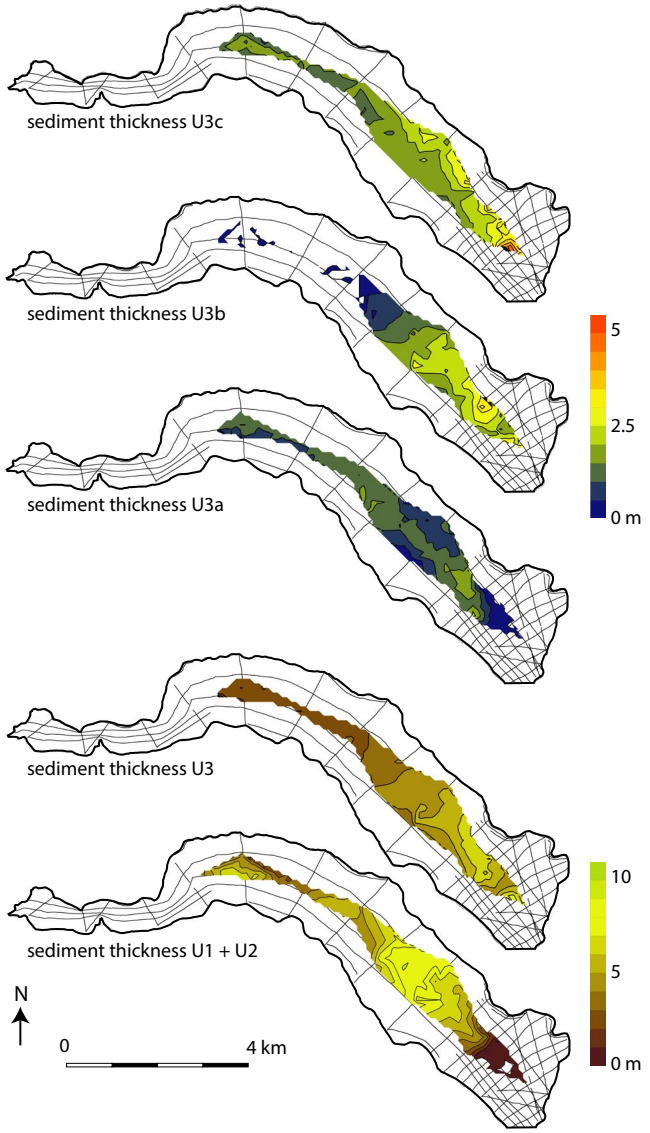

FIGURE 6 Isopach maps of the thickness of units U1, U2 and U3 and subunits U3a, b, and c based on data interpolation. See text for further explanation

internal reflectors. In some locations such as in the mouth of Glomsdalen, the internal reflectors dip *ca* 0.9° lakewards, suggesting local glacio-deltaic deposits.

- Considering the internal seismic properties of unit U2, it is interpreted as an event bed that can be traced across the entire basin. Previous studies correlate this unit with the debris that accumulated following the Storegga tsunami event of 8150 cal yr BP (Vasskog *et al.*, 2013, Figure 4). It is therefore suggested that the undulating lower boundary of this unit corresponds to an erosional surface.

According to Vasskog *et al.* (2012, 2013), sediment overlying the Storegga event bed was deposited under full lacustrine conditions. In unit U3 this is reflected by the consistently parallel nature of the reflectors. Unlike the inclined reflectors characteristic of deposition by slope failure and associated turbidity currents reported from similar nearby lacustrine systems (Vasskog *et al.*, 2011), the parallel reflectors reveal a draping stacking pattern that is traditionally interpreted as indicating settling-dominated depositional processes.

6 | MODELLING WIND-INDUCED LAKE CIRCULATION

Discussed below are the possible mechanisms behind the changing sedimentation patterns identified in subunits U3a–3Uc by modelling current and sediment transport patterns in the lake. This approach applies a coupled hydrodynamic model (Delft3D) to evaluate the effects of river discharge and wind on dispersal patterns of the lake sediments.

6.1 | Analyses of thickness variability based on hydrodynamic modelling

Hydrodynamic modelling is a technique that contributes to a better understanding of the palaeo currents for a given set of boundary conditions. The seismic data has been used to construct the lake bathymetry. The environmental conditions will have changed during the Holocene, as the catchment area shifts from fully glaciated to non-glaciated conditions and back to glaciated. These shifts will have affected the fluvial discharge (water and sediment load) and the local weather system. Wind is an important driver of lake circulation (Krist and Schaetzl, 2001; Nutz *et al.*, 2015; Nutz *et al.*, 2016; Schuster and Nutz, 2018). Given a source of suspended sediment (River Erdalen and the nearby streams), the circulation pattern in the lake determines the mode and fashion the suspended sediments settle. Here, hydrodynamic modelling is used to explain the observed depositional patterns in Lake Strynevatnet as well as the possible causes of variations in relative thickness. It is not possible to reproduce the absolute sediment thicknesses due to a lack of core data from the deep basin.

In addition to discharge, wind is a potential driver of lake circulation (Krist and Schaetzl, 2001; Nutz *et al.*, 2015; Nutz *et al.*, 2016; Schuster and Nutz, 2018). Because Lake Strynevatnet is bordered by steep valley walls (>1,000 m), local winds at the lake surface are expected to originate either from the south-east or from the west–north-west (Figure 3). Hydrodynamic modelling is then used to test the impact of lake currents due to variabilities in wind strengths and directions. It can be assumed that the wind strength may have varied between full glacial and non-glacial intervals. This is especially true with katabatic winds during glacial periods, which may have been distinctly different from non-glacial conditions. Katabatic winds consisting of cold air would have run down Hjelledalen, Sunndalen and Erdalen as the valley confined winds would

have been funnelled and amplified across the surface of Lake Strynevatnet. Furthermore, the western winds may also have changed in intensity during the Late Holocene.

It is hypothesized that changes in discharge and/or wind will affect the currents in lakes Strynevatnet and Nerfloen. Complex currents will affect the sediment concentration patterns and the water mixing rate, thereby potentially affecting the sedimentation pattern at the lake floor. To test this hypothesis, a full 3D coupled hydrodynamic and sediment transport model was applied to simulate the water and sediment flow under different generic wind and discharge conditions.

6.2 | Delft3D model setup

The absence of clearly identified past input conditions inhibits the construction of a valid model. Boundary input values were assumed and model applications were approached in a qualitative, rather than quantitative fashion (main parameters used are summarized in Tables 1 and 2). As such, three generic scenarios with varying wind forces were designed to test hypotheses. The selected palaeowind conditions represent a realistic range in potential wind forces and directions. By adding suspended sediments to the fluvial input boundary, it is possible to describe the lacustrine sediment dynamics, mixing of the water column and sediment trapping efficiency for all three wind scenarios. In addition, by defining two grain-size fractions with different settling velocities it becomes possible to evaluate if the grain sizes of the suspended sediments play a role in the sedimentation patterns of the lake. The generic Delft3D model setup includes the lake bathymetry (Figure 3) and a simplified setup for river inflow that includes the total discharge of all four streams entering the lake from the south-east.

TABLE 1 Delft3D input parameters

Parameter	Value	Unit	Comment
Sediment settling velocity clay	0.005	mm/s	
Sediment settling velocity silt	0.01	mm/s	
Critical shear stress for erosion	0.5	N/m^2	Silt and clay
Initial sediment thickness at the bed	0.05	m	Silt
Cell dimension	100 × 100	m	
Model domain	125 × 67 × 20	voxels	
Bottom roughness coefficient	65	$m^{½}/s$	Chezy formulation
Input boundary type	Discharge	—	
Outflow boundary type	Water level	—	
Number of vertical layers in water column	20	—	
Composition basin floor	Silt	—	
Simulation time	1	year	
Simulation time step	30	s	
Morphological scaling factor	2	—	

TABLE 2 Model scenario parameter setup. Both wind magnitudes and directions are illustrated in Figure 6

	Scenario			
Parameter	1a	1b	2	3
Fluvial water discharge (m^3/s)	60	600	60	60
Sediment discharge clay (kg/m^3)	0.1	0.1	0.1	0.1
Sediment discharge silt (kg/m^3)	0.1	0.1	0.1	0.1
Wind velocity m/s (see Figure 6)	0	0	0.3–7.0	1.5–35.0

The effect of discharge on the lake circulation was initially assessed by imposing a water discharge of 60 m^3/s (Scenario 1a) and 600 m^3/s (Scenario 1b) without wind, to assess if discharge alone induced circulation patterns. The imposed discharge values represent a duplication of the present-day peak discharge (60 m^3/s) and a more extreme value, potentially representing deglacial conditions (600 m^3/s). Subsequently, two wind scenarios (Scenarios 2 and 3, see Table 2) were defined with a discharge of 60 m^3/s and a dominant wind direction approximately parallel to the lake axis (Figure 7).

Winds were set to originate from either the east–north-east representing katabatic winds from Jostedalsbreen ice cap, or from the west to north-west reflecting Atlantic winds funnelling through Nordfjord and adjacent fjords. Hence, it was possible to create two artificial daily wind time series using a simple stochastic approach with identical directions but with different magnitudes. The high-wind scenario is characterized by a fivefold increase in wind speed compared to the low-wind scenario.

6.3 | Simulation results and analyses

6.3.1 | Scenario 1

With no winds (Scenario 1), only minor currents were generated in Lake Strynevatnet near the inflow and outflow areas of the fluvial systems (Figure 8A). A similar interpretation can be obtained from the cross-sections. Here, generated currents are minor at all modelled water depths with an overall direction towards the lake outlet (Figure 8B,C). To evaluate the sensitivity of the model to fluvial

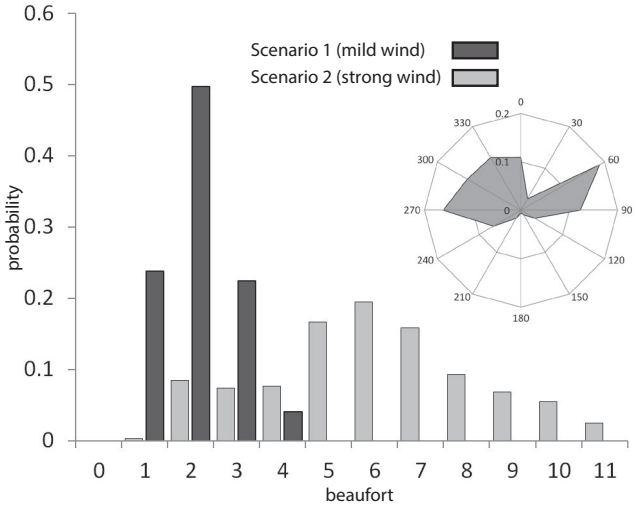

FIGURE 7 Synthetic wind climate as used for hydrodynamic modelling to understand the current patterns in Lake Strynevatnet under different wind conditions. The rose diagram (inset) shows the probability for the wind direction, which is similar for the low-wind and high-wind scenarios

discharge the imposed fluvial discharge was increased by a factor of 10 (600 m^3/s). However, the results indicate that the increased discharge by itself did not produce a circulation pattern in the lake. The main reason for this is that the discharge at the outflow point has a similar capacity as the discharge at the inflow point, preventing the evolution of complex circulation patterns. A poorly mixed water column was probably generated, with sediment concentrations for both clay and silt increasing with water depth (Figure 8A,J). Therefore, the simulations show that fluvial discharge alone is insufficient to create lacustrine circulation patterns.

6.3.2 | Scenario 2

The mild wind conditions of Scenario 2 resulted in a moving water mass, local downwelling and upwelling and contrasting flow directions for shallow and deep sections of the lake (Figure 8D through F). For example, after 24 h of east–south-east wind (100° at 4.0 m/s) at day 197 of the simulation, the modelled average flow velocities are well below 0.05 m/s (Figure 8E). A clear 3D circulation pattern emerges with vertical (Figure 8E) and lateral currents (Figure 8F). Two different flow regimes occur at depth: (a) an upper current towards the west–north-west (similar to the modelled wind direction at that time), and (b) a return current towards the south-east below water depths of approximately 50 m. Downwelling occurs along the southern shores and upwelling along the northern shore at the location of the cross-section. The upwelling and downwelling, as well as the return flow, change direction if the wind direction alternates to a western wind. As a result of the complex flow pattern during the low to moderate wind events of Scenario 2, the water mass is fairly well mixed and concentrations vary little with depth (Figure 8J). However, during periods of low wind activity, the degree of water and sediment mixing decreases.

6.3.3 | Scenario 3

Scenario 3 overall shows a similar behaviour of the water mass under the strong wind conditions (wind from the west at 20 m/s) computed for scenario 2, yet the flow velocities are significantly higher (Figure 8G through I). The downwelling is also more pronounced with much higher overall flow velocities ranging from 0.3 m/s at the surface to 0.1–0.2 m/s at depth. Furthermore, the boundary between the shallow and return flows occurs at approximately 25–30 m water depth. Near Lake Nerfloen, where the water depth is much less, a more local and complex flow pattern evolves (Figure 7G). The sediment concentrations (Figure 8J) are higher than for Scenario 2 and constant with depth, suggesting a well-mixed water body.

It is noteworthy that in Scenario 3 the modelled silt concentration exceeds the clay concentration in Lake Strynevatnet, while the reverse is observed in Scenarios 1 and 2.

6.3.4 | Simulated time-series analyses

Time-series analyses of the simulated scenarios show that the lake water body reacts quickly to a shift in wind conditions. Within 3–5 h (depending on the magnitude of the shift), a new circulation pattern is established.

At the Nerfloen outflow point, the sediment concentrations for both the clay and silt sediment class increase over time for all scenarios (Figure 9). An equilibrium concentration will likely evolve over time as a function of the inflow concentration, the average residence time of the water in Lake Strynevatnet and the sediment setting velocity. The modelling scenarios were not designed to quantify this equilibrium concentration, yet Figure 9 shows that after 365 days, this concentration is not yet reached. Furthermore, the modelling results show that Lake Strynevatnet is not a perfect sediment trap. Suspended sediment is able to escape from the lake while being transported towards Nordfjord. This has an implication for the Holocene sediment yield reconstruction.

The time-series of silt concentration for Scenario 3 (Figure 9) does not follow the same trend as for clay sediment concentration, but it shows strong increases and decreases over short

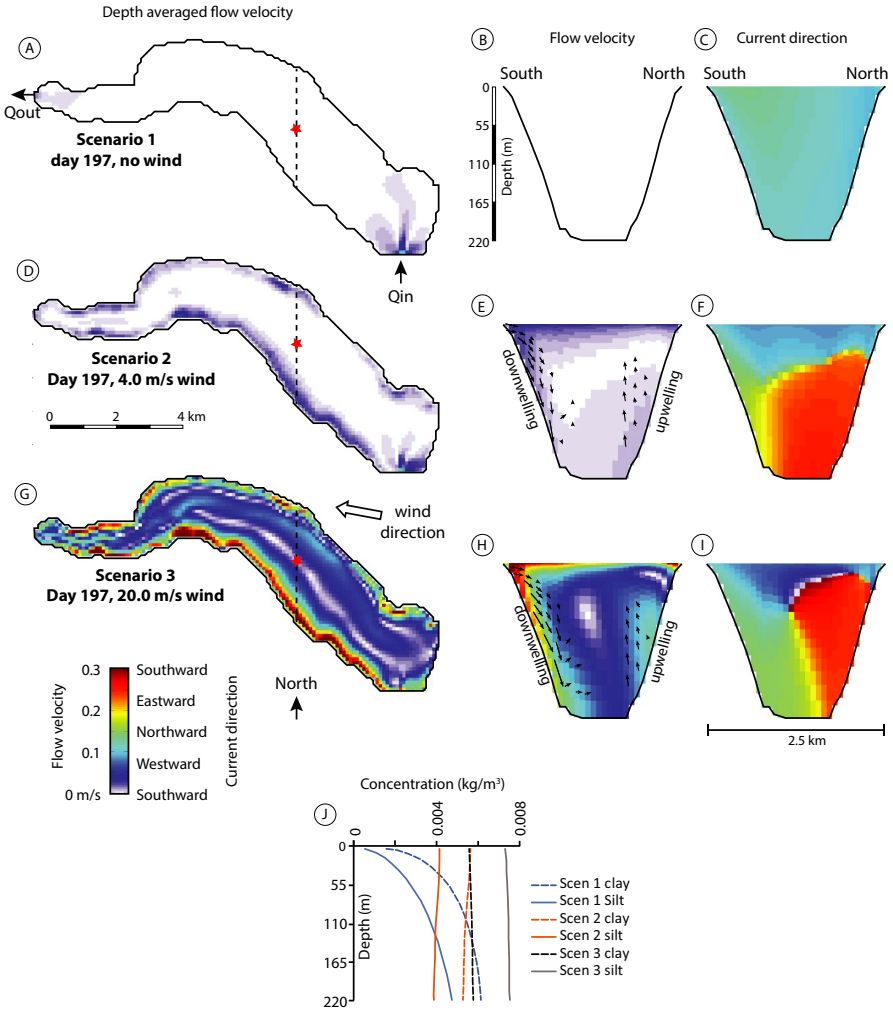

FIGURE 8 Results of the simulations using Delft3D showing depth averaged flow velocities (A, D and G) and vertical flow velocities in cross-section (B, E and H), and the associated current directions (C, F, I). (J) The sediment concentration profiles at the centre of the cross-sections (B, E and H), annotated with a red star. These results represent a snap shot in time (day 197) where the wind has been blowing for 24 h from the east–south-east at 4 m/s (Scenario 2) and from the same direction at 20 m/s for Scenario 3. (E) and (H) show upwelling and downwelling patterns

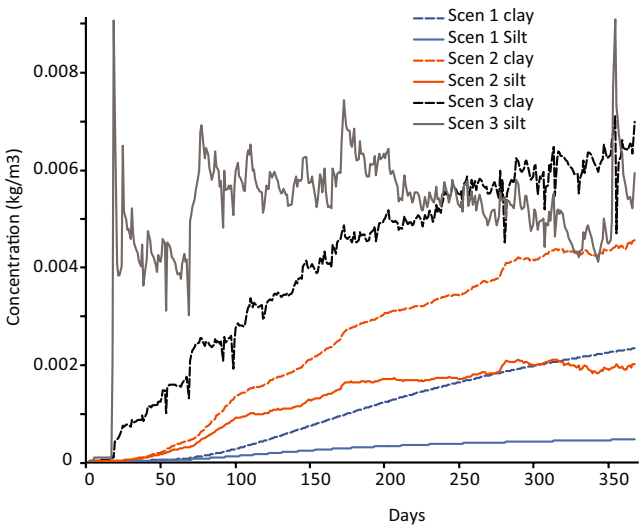

FIGURE 9 Time series of modelled sediment concentrations for the three scenarios and both sediment fractions near the Lake Nerfloen outflow point

time intervals. Further analyses of the simulation data revealed that there were 12 wind events in Scenario 3 that led to strong flow velocities in the shallow part of Lake Nerfloen, which gave rise to minor erosion of the lake floor (Figure 10). Erosion ranged between <0.1 and 6 mm per event, depending on the wind conditions and on the location in the lake. Erosion occurred for storms originating from both western and eastern directions.

As only silt is defined as lake floor sediment (Table 1), erosion will only affect the silt concentration in the water column. The re-suspended silt is drawn into Lake Strynevatnet by the circulation patterns originating from both western and eastern winds. The effective mixing of the water body is rapidly reflected in the silt concentration across Lake Strynevatnet (Figure 10). Within a day, the silt concentrations in the lake centre and near the Erdalen effluent respond to the erosion event in Lake Nerfloen. The silt concentration curve in the lake centre is quite smooth as mixing of the water body is highest at this location. Near the Erdalen effluent, the silt concentration curve is more volatile due to changes in the wind direction with time that affects the local mixing rate of fluvial derived and lake waters.

The simulated sediment accumulated rates for Scenarios 1–3 are plotted in Figure 11. A clear proximal to distal trend in sediment accumulation rate arises for Scenarios 1 and 2, where the rates are highest near the Erdalen effluent.

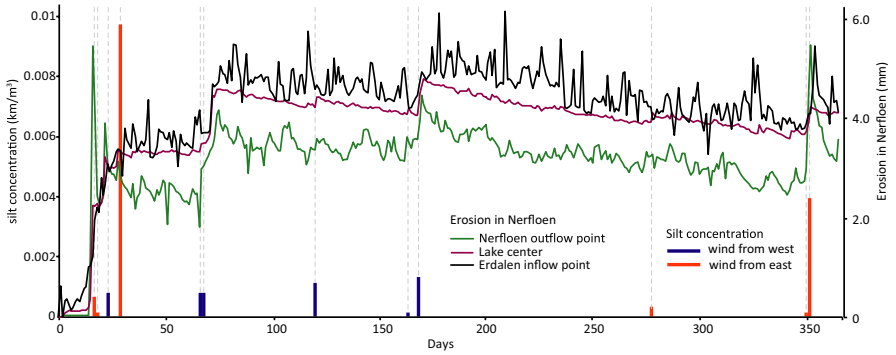

FIGURE 10 Time series of modelled silt concentrations for Scenario 3 at three locations in Lake Strynevatnet. Blue and orange bars indicate the timing and magnitude of erosion events in Lake Nerfloen, as well as the wind direction associated with the erosion event. The lake depocentre location refers to the red star in Figure 8A

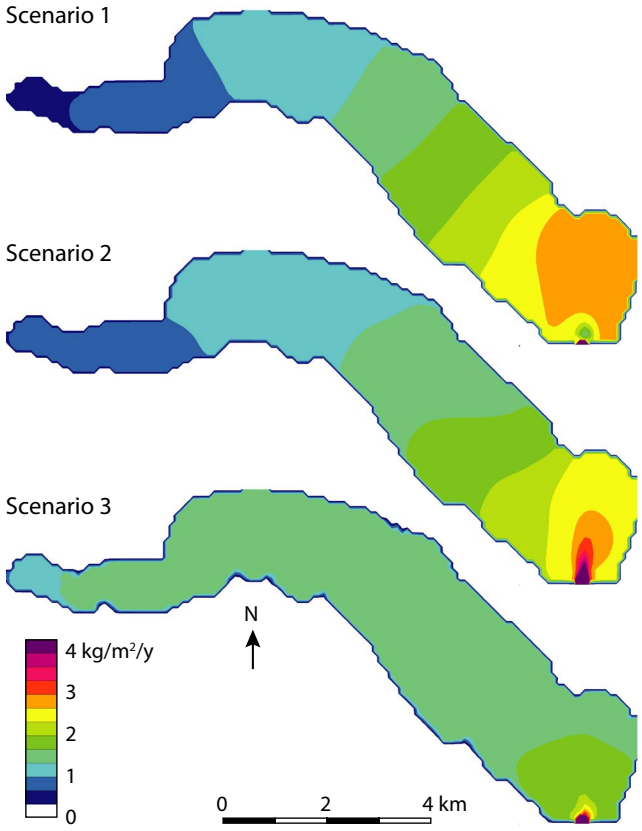

FIGURE 11 Simulated cumulative sediment accumulation in Lake Strynevatnet after one simulation year using Delft3D. The patterns show a clear shift from a proximal to distal decrease in sedimentation for no wind and low-wind conditions, while the strong wind conditions generate a uniform sediment thickness

The absence of wind-driven lake circulation patterns for Scenario 1 leads to higher proximal deposition rates and lower distal deposition rates. This trend in deposition rate also occurs in Scenario 2, but compared to Scenario 1, more sediment is deposited in the distal (western) area of Lake Strynevatnet. Wind-induced circulation patterns in the lake affect the deposition pattern, but not to the extent that the proximal to distal trend is overprinted. For Scenario 3 it is evident that the many wind-events that occur during the year have fully overprinted the proximal to distal trend resulting in more homogeneous sediment accumulation rates across the lake.

6.3.5 | Estimated trapping efficiency

The absolute trapping efficiency of Lake Strynevatnet for suspended sediment is unknown. The numerical simulations do, however, provide a first estimate of the trapping efficiency for the three scenarios as the supplied and preserved sediment volume can be directly compared. The simulated sediment trapping efficiencies for Scenarios 1–3 over the final 2 months of the simulated year are respectively 0.82, 0.76 and 0.68. The trapping efficiency for Scenarios 1–3 for clay only are respectively 0.72, 0.65 and 0.61 and for silt 0.93, 0.87 and 0.74. The numbers show that the trapping efficiency is higher for silt than for clay sediments and that the trapping efficiency decreases with the strength of the wind-induced currents. Over time, it is likely that the simulated trapping efficiency decreases further as Figure 9 shows that the sediment concentrations at the outflow point of Lake Strynevatnet are still rising towards the end of the simulation.

7 | RECONSTRUCTED SEDIMENT YIELD FOR UNIT U3

The average suspended sediment yield can be calculated based on the reconstructed sediment volumes interpreted from the geophysical data. In order to do that, we need to assume a dry-bulk sediment density and a sediment trapping efficiency. Vasskog *et al.* (2012) reported a sediment dry-bulk density in Lake Nerfloen, the shallow extension of Lake Strynevatnet, ranging between 400 and 700 kg/m^3, for sediments overlying the Storegga events (see fig. 3 in Vasskog *et al.*, 2012). In the absence of direct dry-bulk sediment density measurements in Lake Strynevatnet, this study uses the average value of the measured dry-bulk sediment density value of 517 kg/m^3 based on values reported by Vasskog *et al.* (2012). This average value is in agreement

with the dry-bulk density estimates based on granulometric measurements of fine silt to clay (Verstraeten and Poesen, 2001) and falls within the range of dry bed sediment densities for Drammensfjord (250–700 kg/m^3; Smittenberg *et al.*, 2005). In addition, it is necessary to correct the mapped sediment volumes of unit U3 for the trapping efficiency of the suspended sediment in Lake Strynevatnet. The estimated trapping efficiency of 0.7 is slightly lower than the calculated value for Scenario 2 which represents clay and silt combined, as suspended sediment concentrations at the outflow point of Lake Strynevatnet are still rising (Figure 9).

In order to calculate the sediment yield for unit U3, a catchment area of 440 km^2 is used, representing all catchments of Lake Strynevatnet (Figure 1). Based on the above assumptions regarding dry-bulk density and trapping efficiency, it is estimated that since 8150 cal yr BP, 5.0 t/km^2/year of sediment has been supplied to Lake Strynevatnet.

The contemporary suspended sediment yield values for Erdalen valley (16.4 t/km^2/year; Beylich *et al.*, 2017) appear to be much higher than the overall value of the past 8150 years. This might suggest that the current glacier retreat results in a higher sediment yield than that obtained over the past 8150 years, which includes a glacier-free period. Compared to other partly glaciated drainage basin systems in Norway and in other cold climate environments worldwide, the contemporary suspended sediment yield measured for Erdalen is rather low (Beylich *et al.*, 2017).

8 | DISCUSSION

This study indicates the value of combining detailed mapping of lake infill sediments and a thorough understanding of the associated hydrodynamic processes in the lake. The variability in hydrodynamic processes can be better understood by utilizing numerical process models, assuming there is a basic bathymetric map available. The seismic lake infill characterization serves as quality control of the numerical process models. The ongoing challenge is how to operate these numerical models in the absence of any hydrodynamic monitoring data to validate and calibrate model parameters. There are still many lakes in the world where we lack a basic bathymetric map and have no insight into the sediment infill, nor are there any hydrodynamic observations or monitoring data. Global climate models can provide us with some general climate data on precipitation, temperature and wind which may be enough to improve our understanding of lake hydrodynamics and associated morphodynamics. Yet in order to assess the results of the hydrodynamic models there needs to be an understanding of the lake bathymetry and sediment infill.

Specifically, for lakes that are under threat of future climate change (including the effects of lake-level variations, and variations in sediment and water discharge), in combination with an overall increasing human population and associated dependency on lake resources (fresh water, fish farming, irrigation, etc.) a combination of numerical modelling and geophysical characterization (which are both low-cost) will provide valuable insight into lake hydrodynamics which will benefit future management of lake waters.

The geophysical data presented in this paper show that unit U3 consists of three subunits with clearly differentiated stratigraphic signatures. The Delft3D simulation data provide a qualitative explanation for such observed trends related to wind patterns and wind-induced currents. Sediment distribution observations for subunits U3a–U3c suggests a pattern of alternating strong and weak wind conditions. Vasskog *et al.* (2012) discussed the presence of distinct glacial and non-glacial conditions during the past 8000 years in the catchment area of Lake Strynevatnet. In the absence of a core and absolute age dating of the three subunits, it is only possible to speculate whether the formation of subunits U3a-3Uc are related to the variable Holocene glacial conditions of Jostedalsbreen (Nesje *et al.*, 1991; Nesje and Kvamme, 1991) and related Holocene regional climate variability (Karlén and Kuylenstierna, 1996). Palaeoclimate reconstructions typically address past temperature and precipitation patterns yet provide very little information on palaeowind conditions. This study shows that changes in wind patterns (either originating from the Atlantic side or katabatic in origin) will clearly affect lake depositional patterns, which provides an as yet untapped potential stratigraphic archive that can contribute to an improved understanding of palaeoclimate (Krist and Schaetzl, 2001; Nutz *et al.*, 2015; Nutz *et al.*, 2016; Schuster and Nutz, 2018).

The numerical model study only focused on simulating wind-induced currents, the associated spatial and temporal sediment concentrations and the resulting sediment accumulation thickness, ignoring potential complicating factors such as mass failures along the steep lake valley walls, hyperpycnal events or density driven currents, temperature induced lake circulation or the effects of surface ice on lake circulation. The model returned qualitative results and allowed the wind to be identified as an important force that clearly affects the depositional patterns in the lake. It also shows that winds from both directions have a similar effect on the lake circulation. In addition, it has become evident that erosion resulting from wind-induced currents must have affected the shallow Lake Nerfloen confirming the findings of Vasskog *et al.* (2012).

9 | CONCLUSIONS

- The present study combines geophysical data and numerical model data to increase our understanding of

palaeocurrent patterns in Lake Strynevatnet.

- Three seismic units and their ages are identified in Lake Strynevatnet. A chronological framework is obtained from other studies (a) unit U1: marine and lacustrine deposits 11000–8150 cal yr BP), (b) unit U2: Storegga-tsunami deposits (8150 cal yr BP), and (c) unit U3: lacustrine deposits (8,150-present). The latter unit can be subdivided into three based on differences in geometry and seismic facies.
- Preserved sediment volumes have been reconstructed for each of the three units and subunits based on the seismic data. The total minimum volume of sediments imaged and mapped in the Strynevatnet Basin is 0.0537 km^3. The sum of unit U1 and U2 represent 55% of the preserved sediment volume (0.0293 km^3) while unit U3 represents 45% of the total sediment volume (0.0244 km^3). Of that latter volume, subunit U3a represents 21%, U3b provides 31% and U3c represents 48%.
- Based on the hydrodynamic modelling results of wind-induced circulation patterns, it is possible to conclude that wind magnitude, not wind direction, affects the sediment dispersal system on the lake floor. Weak winds lead to a typical trend in sedimentation rate from high near the river effluent to low in settings that are more distal. Strong winds are more effective at mixing the upper part of the water column, which results in a homogeneous sedimentation rate across the lake.
- Based on the comparison between the sedimentation pattern in the lake and the hydrodynamic simulation presented here, it is proposed that the glaciation history of Jostedalsbreen has had an impact on the strength of the katabatic winds during the past 8150 years.
- Model results show that the trapping efficiency in Lake Strynevatnet for suspended sediments decreases with modelled wave-induced current velocities in the lake (from 0.82 when the wind is absent to 0.68 for strong winds). Furthermore, trapping efficiency for silt is higher than for clays due to the difference in settling velocities.
- The calculated yield for fine sediment (suspended) is 5.0 t/km^2/year (post 8150 cal yr BP). Measured present-day values are 16.4 t/km^2/year.
- Changes in wind patterns (either originating from the Atlantic side or katabatic in origin) will affect lake depositional patterns, which provide an as yet untapped potential to improve our understanding of palaeoclimates in stratigraphic studies.

ACKNOWLEDGEMENTS

The Dutch Science Foundation NWO financed this research through the International Polar Year grant scheme (grant number ALW-NAP/08-06). We would like to thank Marcella Schoenmaker for her seismic interpretation work (BSc project), Adriaan Janszen and Ilja de Winter for their field assistance, Alber Hemstede† for his technical support, Dirk Jan Walstra (Deltares) for the hydrodynamic modelling support, and Roderik Lindenbergh TU Delft for his advice on various interpolation methods. We highly appreciated the constructive reviews by Editor in Chief PeterSwart, Associate editor Paul Carling and two anonymous reviewers.

CONFLICT OF INTEREST

The authors have no conflict of interest to declare.

DATA AVAILABILITY STATEMENT

The raw seismic data, GPS positions and Delft3D simulation input used in this study can be freely accessed at: https://doi.org/10.4121/uuid:84e8116b-d866-474d-963a-129c0a341555

ORCID

Joep E. A. Storms https://orcid.org/0000-0002-8902-8493

REFERENCES

Aarseth, I. (1997) Western Norwegian fjord sediments: age, volume, stratigraphy and role as temporary depository during glacial cycles. *Marine Geology*, *143*, 39–53. https://doi.org/10.1016/S0025-3227(97)00089-3.

Aarseth, I., Lønne, Ø. and Giskeødegaard, O. (1989) Submarine slides in glaciomarine sediments in some Western Norwegian fjords. *Marine Geology*, *88*, 1–21. https://doi.org/10.1016/0025-3227(89)90002-9.

Beylich, A.A. and Laute, K. (2012) Spatial variations of surface water chemistry and chemical denudation in the Erdalen drainage basin, Nordfjord, western Norway. *Geomorphology*, *167–168*, 77–90. https://doi.org/10.1016/j.geomorph.2012.03.030.

Beylich, A.A. and Laute, K. (2015) Sediment sources, spatiotemporal variability and rates of fluvial bedload transport in glacier-connected steep mountain valleys in western Norway (Erdalen and Bødalen drainage basins). *Geomorphology*, *228*, 552–567. https://doi.org/10.1016/j.geomorph.2014.10.018.

Beylich, A.A., Laute, K., Liermann, S., Hansen, L., Burki, V., Vatne, G. *et al*. (2009) Subrecent sediment dynamics and sediment budget of the braided sandur system at Sandane, Erdalen (Nordfjord, Western Norway). *Norsk Geografisk Tidsskrift*, *63*, 123–131. https://doi.org/10.1080/00291950902907934.

Beylich, A.A., Laute, K. and Storms, J.E.A. (2017) Contemporary suspended sediment dynamics within two partly glacierized mountain drainage basins in western Norway, Erdalen and Bødalen, inner Nordfjord). *Geomorphology*, *287*, 126–143. https://doi.org/10.1016/j.geomorph.2015.12.013.

Bondevik, S., Svendsen, J.I. and Mangerud, J. (1997) Tsunami sedimentary facies deposited by the Storegga tsunami in shallow marine basins and coastal lakes, western Norway. *Sedimentology*, *44*, 1115–1131. https://doi.org/10.1046/j.1365-3091.1997.d01-63.x.

Chapron, E., Juvigné, E., Mulsow, S., Ariztegui, D., Magand, O., Bertrand, S. *et al*. (2007) Recent clastic sedimentation processes in Lake Puyehue (Chilean Lake District, 40.5°S). *Sedimentary Geology*, *201*(3–4), 365–385. https://doi.org/10.1016/j.sedgeo.2007.07.006.

Cukur, D., Krastel, S., Çağatay, M.N., Damcı, E., Meydan, A.F. and Kim, S.-P. (2015) Evidence of extensive carbonate mounds and

sublacustrine channels in shallow waters of Lake Van, eastern Turkey, based on high-resolution chirp subbottom profiler and multibeam echosounder data. *Geo-Marine Letters*, *35*, 329–340. https://doi.org/10.1007/s00367-015-0410-x.

Fanetti, D., Anselmetti, F.S., Chapron, E., Sturms, M. and Vezzoli, L. (2008) Megaturbidite deposits in the Holocene basin fill of Lake Como (Southern Alps, Italy). *Palaeogeography, Palaeoclimatology, Palaeoecology*, *259*, 323–340. https://doi.org/10.1016/j.palaeo.2007.10.014.

Haflidason, H., Lien, R., Sejrup, H.P., Forsberg, C.F. and Bryn, P. (2005) The dating and morphometry of the Storegga Slide. *Marine and Petroleum Geology*, *22*, 123–136. https://doi.org/10.1016/j.marpetgeo.2004.10.008.

Hansen, L., Beylich, A.A., Burki, V., Eilertsen, R.S., Fredin, O., Larsen, E. *et al*. (2009) Stratigraphic architecture and infill history of a deglaciated bedrock valley based on georadar, seismic profiling and drilling. *Sedimentology*, *56*, 1751–1773. https://doi.org/10.1111/j.1365-3091.2009.01056.x.

Hillen, M.M., Geleynse, N., Storms, J.E.A., Walstra, D.J.R. and Groenenberg, R.M. (2014) Morphodynamic modeling of wave reworking of an alluvial delta and application of results in the standard reservoir modeling workflow. In Martinius, A.W., Ravnås, R., Howell, J.A., Steel, R.J. and Wonham, J.P. (Eds.), *From Depositional Systems to Sedimentary Successions on the Norwegian Continental Margin*. *International Association of Sedimentologists, Special Publication*, *46*, 167–186. doi:https://doi.org/10.1002/9781118920435.ch8.

Hjelstuen, B.O., Haflidason, H., Sjerup, H.P. and Lysså, A. (2009) Sedimentary processes and depositional environments in glaciated fjord systems - Evidence from Nordfjord, Norway. *Marine Geology*, *258*, 88–99. https://doi.org/10.1016/j.margeo.2008.11.010.

Karlén, B. and Kuylenstierna, J. (1996) On solar forcing of Holocene climate: evidence from Scandinavia. *The Holocene*, *6*, 359–365. https://doi.org/10.1177%2F095968369600600311.

Krist Jr, F. and Schaetzl, R.J. (2001) Paleowind (11,000 BP) directions derived from lake spits in Northern Michigan. *Geomorphology*, *38*, 1–18. https://doi.org/10.1016/S0169-555X(00)00040-4.

Lesser, G.R., Roelvink, J.A., van Kester, J.A.T.M. and Stelling, G.S. (2004) Development and validation of a three-dimensional morphological model. *Coastal Engineering*, *51*, 883–915. https://doi.org/10.1016/j.coastaleng.2004.07.014.

Lysså, A., Hjelstuen, B.O. and Larsen, E. (2010) Fjord infill in a high-relief area: rapid deposition influenced by deglaciation dynamics, glacio-isostatic rebound and gravitational activity. *Boreas*, *39*, 39–55. https://doi.org/10.1111/j.1502-3885.2009.00117.x.

Mullins, H.T., Eyles, N. and Hinchey, E. (1991) High-Resolution Seismic Stratigraphy of Lake Mcdonald, Glacier National Park, Montana, U.S.A. *Arctic and Alpine Research*, *23*, 311–319. https://doi.org/10.1080/00040851.1991.12002850.

Nesje, A. (2009) Latest Pleistocene and Holocene alpine glacier fluctuations in Scandinavia. *Quaternary Science Reviews*, *28*, 2119–2136. https://doi.org/10.1016/j.quascirev.2008.12.016.

Nesje, A. and Kvamme, M. (1991) Holocene glacier and climate variations in western Norway: evidence for early Holocene glacier demise and multiple Neoglacial events. *Geology*, *19*(6), 610–612. https://doi.org/10.1130/0091-7613(1991)019<0610:HGACVI>2.3.CO;2.

Nesje, A., Kvamme, M., Rye, N. and Løvlie, R. (1991) Holocene glacial and climate history of the Jostedalsbreen region, Western Norway: Evidence from lake sediments and terrestrial deposits. *Quaternary Science Reviews*, *10*, 87–114. https://doi.org/10.1016/0277-3791(91)90032-P.

Nesje, A., Dahl, S.O., Andersson, C. and Matthews, J.A. (2000) The lacustrine sedimentary sequence in Sygneskardvatnet, western Norway: a continuous, high-resolution record of the Jostedalsbreen ice cap during the Holocene. *Quaternary Science Reviews*, *19*, 1047–1065. https://doi.org/10.1016/S0277-3791(99)00090-6.

Nutz, A., Schuster, M., Ghienne, J.F., Roquin, C., Hay, M.B., Rétif, F. *et al*. (2015) Wind-driven bottom currents and related sedimentary bodies in Lake Saint-Jean (Québec, Canada). *GSA Bulletin*, *127*, 1194–1208. https://doi.org/10.1130/B31145.1.

Nutz, A., Schuster, M., Ghienne, J.F., Roquin, C. and Bouchette, F. (2016) Wind-driven waterbodies: a new category of lake within an alternative sedimentologically-based lake classification. *Journal of Paleolimnology*, *59*, 189–199. https://doi.org/10.1007/s10933-016-9894-2.

Rye, N., Nesje, A., Lien, R., Blikra, L.H., Eikenæs, O., Hole, P.A. *et al*. (1997) Glacial geology and deglaciation chronology of the area between inner Nordfjord and Jostedalsbreen-Strynefjellet, western Norway. *Norsk Geologisk Tidsskrift*, *77*, 51–63.

Schneider von Deimling, J., Held, P., Feldens, P. and Wilken, D. (2016) Effects of using inclined parametric echosounding on sub-bottom acoustic imaging and advances in burried object detection. *Geo-Marine Letters*, *36*, 113–119. https://doi.org/10.1007/s00367-015-0433-3.

Schuster, M. and Nutz, A. (2018) Lacustrine wave-dominated clastic shorelines: modern to ancient littoral landforms and deposits from the Lake Turkana Basin (East African Rift System, Kenya). *Journal of Paleolimnology*, *59*, 221–243. https://doi.org/10.1007/s10933-017-9960-4.

Smittenberg, R.H., Baas, M., Green, M.J., Hopmans, E.C., Schouten, S. and Sinninghe Damsté, J.S. (2005) Pre- and post-industrial environmental changes as revealed by the biogeochemical sedimentary record of Drammensfjord, Norway. *Marine Geology*, *214*, 177–200. https://doi.org/10.1016/j.margeo.2004.10.029.

Van der Vegt, H., Storms, J.E.A., Walstra, D.J.R. and Howes, N.C. (2016) Can bed load transport drive varying depositional behaviour in river delta environments? *Sedimentary Geology*, *345*, 19–32. https://doi.org/10.1016/j.sedgeo.2016.08.009.

VanRensbergen, P., De Batist, M., Beck, Ch and Manalt, F. (1998) High-resolution seismic stratigraphy of late Quaternary fill of Lake Annecy (northwestern Alps): evolution from glacial to interglacial sedimentary processes. *Sedimentary Geology*, *117*, 71–96. https://doi.org/10.1016/S0037-0738(97)00123-1.

Vasskog, K., Nesje, A., Støren, E.N., Waldmann, N., Chapron, E. and Daniel Ariztegui, D. (2011) A Holocene record of snow-avalanche and flood activity reconstructed from a lacustrine sedimentary sequence in Oldevatnet, western Norway. *The Holocene*, *21*, 597–614. https://doi.org/10.1177%2F0959683610391316.

Vasskog, K., Paasche, Ø., Nesje, A., Boyle, J.F. and Birks, H.J.B. (2012) A new approach for reconstructing glacier variability based on lake sediments recording input from more than one glacier. *Quaternary Research*, *77*, 192–204. https://doi.org/10.1016/j.yqres.2011.10.001.

Vasskog, K., Waldmann, N., Bondevik, S., Nesje, A., Chapron, E. and Ariztegui, D. (2013) Evidence for Storegga tsunami run-up at the head of Nordfjord, Western Norway. *Journal of Quaternary Science*, *28*, 391–402. https://doi.org/10.1002/jqs.2633.

Verstraeten, G. and Poesen, J. (2001) Variability of dry sediment bulk density between and within retention ponds and its impact on the calculation of sediment yields. *Earth Surface Process and Landforms*, *26*, 375–394. https://doi.org/10.1002/esp.186.

Waldmann, N., Ariztegui, D., Burki, V., Chapron, E., Hansen, L., Larsen, E., Lyså, A. and Nesje, A. (2007). Linking marine and terrestrial records in the Nordfjord region, western Norway. 4th International Limnogeology Congress (ILIC2007), Barcelona, Spain.

Waldmann, N., Ariztegui, D., Anselmetti, F.S., Coronato, A. and Austin Jr, J.A. (2010) Geophysical evidence of multiple glacier advances in Lago Fagnano (54S), southernmost Patagonia. *Quaternary Science Reviews*, *29*, 1188–1200. https://doi.org/10.1016/j.quascirev.2010.01.016.

Wunderlich, J. and Muller, S. (2003) High-resolution subbottom profiling using parametric acoustics. *International Ocean Systems*, *7*, 6–11.

How to cite this article: Storms JEA, Beylich AA, Hansen L, Waldmann N. Source to sink reconstruction of a Holocene Fjord-infill: Depositional patterns, suspended sediment yields, wind-induced circulation patterns and trapping efficiency for Lake Strynevatnet, inner Nordfjord, Norway. *Depositional Rec*. 2020;6:471–485. https://doi.org/10.1002/dep2.101